

APPLYING DIFFERENT MACHINE LEARNING TECHNIQUES FOR PREDICTION OF COVID 19 SEVERITY

K.Surekha¹, E.Ramya², K.Manisha³, M.Nithisha⁴, M.ManuPriya⁵

*1Assistant Professor, Department Of ECE., Malla Reddy College Of Engineering For Women.,
Maisammaguda., Medchal., Ts, India (✉surekhakorudu413@gmail.Com)
2, 3, 4, 5 B.TechECE, (19RG1A0473, 19RG1A0480, 19RG1A0498, 19RG1A04A3),
Malla Reddy College Of Engineering For Women., Maisammaguda., Medchal., Ts, India*

ABSTRACT

Researchers are working feverishly to discover technology solutions to aid physicians in their everyday job as the number of people dying from SARS-Cove 2 increases throughout the globe. To better forecast a patient's severity and mortality risk and aid clinicians in making treatment choices, fast and accurate Artificial Intelligence (AI) solutions are required. Hospitals and healthcare providers might save money and prevent needless patient deaths if their severity assessments were more accurate. X-rays are now utilized as early symptoms for identifying people with COVID-19. As a result, a prediction model has been developed in this study to make risk assessments for the COVID-19 patient using X-ray images and machine learning. The proposed model was constructed using a CheXNet deep pre trained model and hybrid handcrafted techniques for feature extraction, two methods for selecting the most relevant features—Principal Component Analysis (PCA) and Recursive Feature Elimination (RFE)—that were combined, and finally six machine learning methods. The trials showed that the best results were attained across all classifiers when combining the features determined using principal component analysis (PCA) and robust feature extraction (RFE) (PCA+RFE) for the handmade features.

KEY WORDS :

Chest X-rays, COVID-19, deep learning, handcrafted methods, machine learning, mortality forecasting, and severity forecasting are all terms that may be found in the index.

INTRODUCTION

Predicting the severity risk of any illness at an early stage is an important undertaking with numerous impacts, including lowering the mortality rate, decreasing the use of hospital resources, and aiding in the decision-making of clinicians. According to data from Johns Hopkins University [1], the number of COVID-19 patients has reached nearly 217.5 million, while the number of deaths around the world has reached 4.5 million in the critical period during the spread of coronavirus around the world and the increasing number of patients and deaths. The United States is at the top of the list, followed by a long list of other nations like Brazil, India, France, Russia, Italy, and many more. The high frequency of COVID-19, delayed diagnosis, and a lack of resources at many institutions are to blame for this exponential rise in cases. Therefore, predicting the severity risk of COVID-19 patients is an important task with many positive outcomes, such as ensuring that each patient receives the

appropriate level of care for his severity, making efficient use of hospital resources by giving top priority to the highest-risk patient, and helping doctors make decisions that will improve the patient's treatment. In order to detect COVID-19, one might employ X-ray pictures, CT scans, or RT-PCR (reverse transcription-polymerase chain reaction). The most effective method, RT-PCR, is prohibitively costly, not offered by many hospitals, and time-consuming to get findings. Consequently, many medical professionals rely on chest X-rays and CT scans for the early diagnosis and treatment of this disease [2]. Normal CT takes from zero to two days to view its findings [3], making CT challenging to employ in periodic monitoring since its results might be noticed after a lengthy time according to the onset of symptoms. Even though it lacks the sensitivity of CT and RT-PCR, chest X-ray (CXR) radiography is still one of the most accessible and widely used methods for a quick examination of lung conditions. Since X-ray findings can be seen in a relatively short amount of time and the method is relatively inexpensive, it can be used on a regular basis to keep tabs on the patient's health.

CONTENT AND APPROACHES

In this part, we lay out the specifics of our proposed model for estimating the impact of COVID-19. The framework's broad design is laid forth first, followed by a discussion of the methods actually used to make severity predictions.

THE PROPOSED ARCHITECTURE

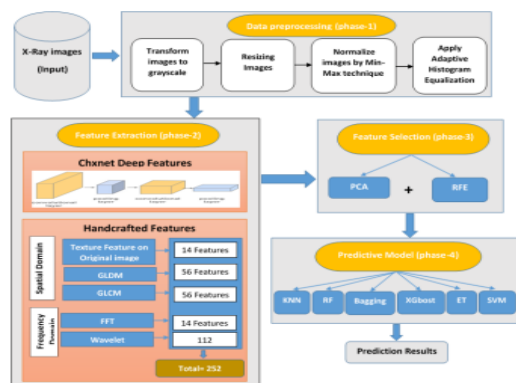


FIGURE 1: The proposed architecture. The proposed framework consists of four main phases, as shown in Fig. 1. Firstly, the input X-ray dataset is passed to data pre-processing to resize and normalize the images. Then, different feature extraction methods are applied to extract the features. After that, feature selection techniques are executed to select the most important features in the images, and finally, different machine learning classifiers are applied to build the models.

SUGGESTIONS FOR A METHOD

In this paragraph, we will quickly go through the suggested framework's primary stages.

Pre-processing the Data

Preparing the data for use in the prediction model is the primary goal of the data pre-processing stage. In most cases, data are unstructured and originate from a variety of sources, each with their own unique format and level of detail. Cleaning and standardizing the data at this stage is thus essential for lowering the prediction model's complexity and raising its precision. Depending on the data set, various operations such as scaling, rotation, and translation might be carried out.

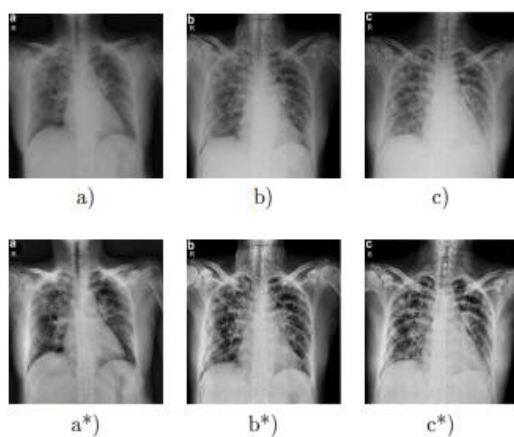


FIGURE 2: (a), (b), and (c) are examples of images before applying the pre-processing methods, while (a*), (b*), and (c*) are examples of images after applying the pre-processing methods.

Typical zing, etc. Following the order shown in Fig. 1, the dataset undergoes the four preparation stages. In order to maximize the radiography information content [26] and better present diagnostically significant information, the picture must first be converted to grayscale. Second, scale the picture to 512x512 for handmade characteristics, as suggested in [16], [27], and [28], to ensure that the most informative data regarding the patient's severity level is preserved. Otherwise, information related to the same assigned class of the whole image may be lost if the image is smaller than 512 pixels on a side. Images should be resized to 224x224 for deep features to ensure they meet the specifications of the Cheyne pre-trained model. Third, adopting Adaptive Histogram Equalization (AHE) to boost contrast and enhance the medical picture after normalizing the image using the min-max approach to rescale the image pixels in the range of 0-1. X-ray pictures are shown before and after the data preparation step in Fig. 2.

next stage is feature extraction.

This study decided to use a pre-trained Cheyne deep model and a set of handcrafted descriptors to extract features from medical images due to the small size of the dataset used and the encouraging results of using the handcrafted techniques and pre-trained models for extracting features from medical images in other published papers [8, 9], [13], [14], [29]-[31]. Deep Functions of CheXNet CheXNet [32] is a 121-layer DenseNet-inspired convolutional neural network study. For 14 types of pneumonia, it learned from over 100,000 chest X-rays taken from the front. CheXNet's efficiency wasIt is believed to have better detection accuracy than the average radiologist when compared to a panel of four academic radiologists who annotated a dataset. Figure 3 provides a high-level overview of the pre-trained CheXNet model that was employed. Features are extracted from X-ray pictures using a network of five convolution blocks and a max-pooling layer. The suggested prediction model makes use of the model's output of 9216 characteristics.

Layer (type)	Output Shape	Param #
input_4 (InputLayer)	[(None, 224, 224, 3)]	0
block1_conv1 (Conv2D)	(None, 224, 224, 64)	1792
block1_conv2 (Conv2D)	(None, 224, 224, 64)	36928
block1_pool (MaxPooling2D)	(None, 112, 112, 64)	0
block2_conv1 (Conv2D)	(None, 112, 112, 128)	73856
block2_conv2 (Conv2D)	(None, 112, 112, 128)	147584
block2_pool (MaxPooling2D)	(None, 56, 56, 128)	0
block3_conv1 (Conv2D)	(None, 56, 56, 256)	295168
..		
block3_conv4 (Conv2D)	(None, 56, 56, 256)	590080
block3_pool (MaxPooling2D)	(None, 28, 28, 256)	0
block4_conv1 (Conv2D)	(None, 28, 28, 512)	1180160
..		
block4_conv4 (Conv2D)	(None, 28, 28, 512)	2359808
block4_pool (MaxPooling2D)	(None, 14, 14, 512)	0
block5_conv1 (Conv2D)	(None, 14, 14, 512)	2359808
..		
block5_conv4 (Conv2D)	(None, 14, 14, 512)	2359808
block5_pool (MaxPooling2D)	(None, 7, 7, 512)	0
re_lu_1 (ReLU)	(None, 7, 7, 512)	0
feature_layer (MaxPooling2D)	(None, 3, 3, 512)	0

FIGURE 3: The summary design of CheXNet model.

PLANS FOR AN EXPERIMENT

This section describes the dataset that was used, the feature selection methods that were used, the machine learning classifiers that were utilized, and the evaluation metrics that were employed.

DATASET

The research made use of a publicly accessible dataset created by Cohen JP [25]. Patients with pneumonia, including those with COVID 19, are represented in the dataset. Patient-id, age, X-ray picture, illness, survival rate, and ICU admission status are all included. The paper's cohort was assembled by first excluding all patients under the age of 18; then choosing only the confirmed COVID-19 patients with a positive RT-PCR test (40 percent female and 60 percent male patients); and finally classifying the patients based on their status indicators (whether they survived or not, and whether or not they were admitted to the intensive care unit). All of these factors are used when classifying patients' degrees of illness. Actually, survival and went-to-ICU variables are the two primary ones used to determine the severity level. If survival is false, the severity is classified as high; if survival and went-ICU are both true, the severity is classified as moderate; and if survival is true and went-ICU is false, the severity is classified as low. The cohort size for these classification criteria is 127 photos, and the highest severity class includes patients at risk of dying, the moderate severity class includes patients who need to join the intensive care unit, and the lowest severity class includes patients with stable conditions who do not need to enter the ICU. To guarantee that all X-ray pictures pertaining to a given patient are distributed to just one (train/test) set, the dataset is divided 80/20 for train/test sets and organized by the patient-id.

TECHNIQUES FOR CHOOSING FEATURES

One) PCA (Principal Components Analysis) The initial data went through the PCA processes described above. Since 24 components account for 95% of the variance in the original data (as shown in Fig. 4), 24 principal components were chosen to represent the handcrafted features. However, CheXNet has 103 components that account for 95% of the variance in the original features, so it has a higher variance ratio.

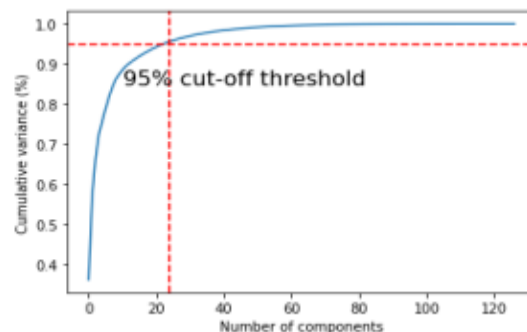


FIGURE 4: The number of PCA components for the handcrafted features.

Feature removal in a recursive fashion for feature selection, two hyperparameters are needed: the target number of features and the objective function method. Gradient boosting, logistic regression, decision trees, random forests, and perceptron's with a wide range of feature sizes have all been attempted. Every feature selection result from these trials has been put through its paces on the machine learning classifiers used here. Because of the countlessOnly the optimal values for the hyper-parameters used to train the classifiers are discussed here; the best estimator algorithm is perceptron, and the optimal number of features is 28 for handcrafted and 100 for CheXNet deep features.

CATEGORIZERS FOR MACHINE LEARNING

The hyper-parameters of the used classifiers were optimized using the grid search algorithm and the trial-and-error method. The utilized classifiers' hyper-parameter values are shown in Table 1.

TABLE 1: Hyper-parameters of each classifier

Classifier	Parameters
KNN	n_neighbors=10.
RF	n_estimators=100; max_depth=6; max_features=0.2.
XGboost	n_estimators=100; learning_rate=0.3; objective=multi:softprob; subsample=0.5.
Bagging	n_estimators=100; base_estimator=DecisionTree; max_features=0.2; max_samples=0.9.
ET	n_estimators=100; max_features=0.2; min_samples_split=15.
SVM	kernel=rbf; C=3; gamma=0.1.

EXPERIMENTAL RESULTS & DISCUSSION

It is worth noting that several experiments have been conducted, but only the most significant ones are reported here because of space constraints. The sklearn package in Python was used to implement the experiments in the research. This package includes libraries for presenting findings, such as a classification report, confusion matrix, roc curve, and area under the curve (AUC). The experiments in section III-A were conducted using the dataset described there. As a starting point, we used the procedures for pre-processing data and extracting features described in sections II-B1 and II-B2.

Then, a number of techniques are used to select features:

- 1) No feature selection techniques were used, hence all retrieved characteristics were utilised.
- (2) Principal Component Analysis is used on the gleaned data.
- 3) the retrieved characteristics are subjected to RFE.
- 4) The characteristics chosen by principal component analysis and robust feature extraction are concatenated (PCA+RFE).

The machine learning classifiers discussed in section III-C were finally put into action. The following tables provide the outcomes of the experiments, with descriptive column headings: Use of all extracted features is indicated by the "All" column, while the "PCA" and "RFE" columns show the outcomes of feature selection using PCA and RFE approaches, respectively, and the "(PCA + RFE)" column displays the outcomes of feature selection using both PCA and RFE techniques. This section is split into two subsections: the first shows the results of the experiments conducted using the features extracted using CheXNet and the second displays the results of the experiments conducted using the features derived using handcrafting.

EXPERIMENTS OVER HANDCRAFTED FEATURES

Table. 2 contains the number of the used handcrafted features in each experiment.

TABLE 2: The number of the used handcrafted features.

Experiment name	Number of features
All	252
PCA	24
RFE	28
PCA + RFE	52

Experiment name Number of features

All 252 PCA 24 RFE 28 PCA + RFE 52 The results in Tables. 3, 4, 5, 6, 7, and 8 demonstrate that using the combined features of PCA and RFE over the handcrafted extracted features achieved the best results on all scores: accuracy, precision, recall, F1-score, and Roc-AUC with all classifiers compared with using all extracted features, PCA features, or RFE features alone. Also, the findings in Tables. 3 and 8 show that using the selected features by PCA was better than using the selected features by RFE with KNN and SVM classifiers respectively. It is appeared that RFE surpassed PCA with the Bagging classifier as described in Table 6, while in the remaining results there were no big differences between using PCA or RFE with ensemble classifiers like Random Forest, XGBoost, and Extra Tree as presented in Tables. 4, 5, and 7 respectively. The compared results in Fig. 5 show that SVM and XGBoost achieved the best accuracy (97%) by using the merged features (PCA+RFE) compared with other classifiers.

TABLE 3: Results of the KNN classifier over the handcrafted features.

Score	All	PCA	RFE	PCA + RFE
Accuracy	0.86	0.90	0.86	0.93
Precision	0.87	0.90	0.87	0.93
Recall	0.81	0.86	0.81	0.90
F1-score	0.83	0.87	0.82	0.90

TABLE 4: Results of the Random Forest classifier over the handcrafted features

Score	All	PCA	RFE	PCA + RFE
Accuracy	0.83	0.86	0.86	0.90
Precision	0.81	0.88	0.88	0.90
Recall	0.79	0.81	0.81	0.86
F1-score	0.80	0.82	0.82	0.87

TABLE 5: Results of the XGBoost classifier over the handcrafted features.

Score	No selection	PCA	RFE	PCA + RFE
Accuracy	0.86	0.90	0.90	0.97
Precision	0.85	0.88	0.91	0.98
Recall	0.86	0.91	0.86	0.95
F1-score	0.85	0.89	0.88	0.96

TABLE 6: Results of the Bagging classifier over the handcrafted features.

Score	All	PCA	RFE	PCA + RFE
Accuracy	0.79	0.76	0.83	0.93
Precision	0.82	0.79	0.81	0.93
Recall	0.74	0.67	0.79	0.90
F1-score	0.76	0.69	0.79	0.90

TABLE 7: Results of the ET classifier over the handcrafted features

Score	All	PCA	RFE	PCA + RFE
Accuracy	0.86	0.90	0.90	0.93
Precision	0.88	0.90	0.91	0.93
Recall	0.83	0.86	0.86	0.90
F1-score	0.83	0.87	0.86	0.90

TABLE 8: Results of the SVM classifier over the handcrafted features

Score	All	PCA	RFE	PCA + RFE
Accuracy	0.90	0.93	0.90	0.97
Precision	0.90	0.93	0.90	0.96
Recall	0.88	0.90	0.86	0.95
F1-score	0.87	0.90	0.87	0.95

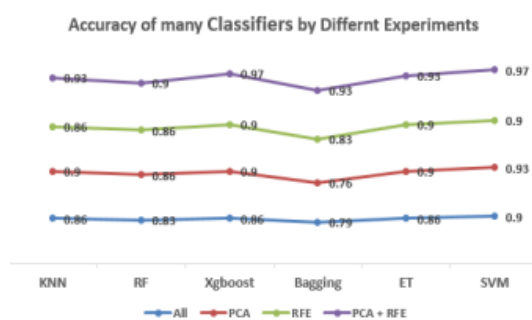


FIGURE 4: The accuracy of the used classifiers by different experiments over the handcrafted features.

The True Positive (TP), True Negative (TN), False Positive (FP), and False Negative (FN) values for each classifier are shown in detail in Figs. 6 and 7, which illustrate the confusion matrices of SVM and XGBoost classifiers. Furthermore, as shown in Figures 8 and 9, the Roc-AUC results of the same classifiers are optimal across all classes.

CONCLUSIONS

In order to aid physicians, hospitals, and other medical facilities in deciding which patients require priority care and which do not, this study proposes a new predictive framework for the severity and mortality risk of COVID-19 patients. The suggested model is based on a publicly available X-ray imaging dataset for patients diagnosed with COVID-19. High, moderate, and low severity categories are used to categorize the dataset. Patients in the highest severity category are at risk of death; those in the moderate category will likely spend time in the intensive care unit (ICU); and those in the lowest category won't need such care. Extraction of features from X-ray images was performed using pre-trained deep CheXNet and hybrid handcrafted techniques; PCA and RFE were then combined as a feature selection method; and many predictive models were constructed using machine learning algorithms such as KNN, Random Forest (RF), XGboosting, Bagging, Extra Tree, and SVM for validation and comparison. Extensive testing showed that, for manually crafted features, the best results could be obtained across all classifiers by merging the selected features using principal component analysis and robust feature extraction (PCA+RFE), with a total of 52 features being used (representing nearly 25% of the original number of extracted features, 252

REFERENCES

- [1] "COVID-19 Dashboard by the Center for Systems Science and Engineering (CSSE) at Johns Hopkins University (JHU)." [Online]. Available: <https://coronavirus.jhu.edu>
- [2] Z. Y. Zu, M. D. Jiang, P. P. Xu, W. Chen, Q. Q. Ni, G. M. Lu, and L. J. Zhang, "Coronavirus disease 2019 (COVID-19): a perspective from China," *Radiology*, vol. 296, no. 2, pp. E15–E25, Feb. 2020.

[3] A. Bernheim, X. Mei, M. Huang, Y. Yang, Z. A. Fayad, N. Zhang, K. Diao, B. Lin, X. Zhu, K. Li et al., "Chest CT findings in coronavirus disease-19 (COVID-19): relationship to duration of infection," *Radiology*, Feb. 2020, Art. no. 200463, DOI: <https://doi.org/10.1148/radiol.2020200463>.

assist in the diagnosis of COVID-19 infection in chest X-ray images," *Sci. Rep.*, vol. 11, no. 1, pp. 1–6, May 2021.

[4] L. Wang, Z. Q. Lin, and A. Wong, "COVID-net: A tailored deep convolutional neural network design for detection of covid-19 cases from chest X-ray images," *Sci. Rep.*, vol. 10, no. 1, pp. 1–12, Nov. 2020.

[5] T. Ozturk, M. Talo, E. A. Yildirim, U. B. Baloglu, O. Yildirim, and U. R. Acharya, "Automated detection of COVID-19 cases using deep neural networks with X-ray images," *Comput. Biol. Med.*, vol. 121, June 2020, Art. no. 103792, DOI: <https://doi.org/10.1016/j.compbimed.2020.103792>.

[6] A. I. Khan, J. L. Shah, and M. M. Bhat, "Coronet: A deep neural network for detection and diagnosis of COVID-19 from chest X-ray images," *Comput. Methods Programs Biomed.*, vol. 196, Nov. 2020, Art. no. 105581, DOI: <https://doi.org/10.1016/j.cmpb.2020.105581>.

[7] M. Rahimzadeh and A. Attar, "A modified deep convolutional neural network for detecting COVID-19 and pneumonia from chest X-ray images based on the concatenation of Xception and ResNet50V2," *Inform. Med. Unlocked*, vol. 19, 2020, Art. no. 100360, DOI: <https://doi.org/10.1016/j.imu.2020.100360>.

[8] N. Habib, M. M. Hasan, M. M. Reza, and M. M. Rahman, "Ensemble of CheXNet and VGG-19 Feature Extractor with Random Forest Classifier for Pediatric Pneumonia Detection," *SN Comput. Sci.*, vol. 1, no. 6, pp. 1–9, Oct. 2020.

[9] P. R. Bassi and R. Attux, "A deep convolutional neural network for COVID-19 detection using chest X-rays," *Res. Biomed. Eng.*, pp. 1–10, Apr. 2021.

[10] J. P. Cohen, L. Dao, K. Roth, P. Morrison, Y. Bengio, A. F. Abbasi, B. Shen, H. K. Mahsa, M. Ghassemi, H. Li et al., "Predicting COVID-19 pneumonia severity on chest X-ray with deep learning," *Cureus*, vol. 12, no. 7, Jul. 2020, DOI: [10.7759/cureus.9448](https://doi.org/10.7759/cureus.9448).

[11] D. Camilleri and T. Prescott, "Analysing the limitations of deep learning for developmental robotics," in *Biomimetic and Biohybrid Systems*, Springer. Cham: Springer, 2017, pp. 86–94, DOI: https://doi.org/10.1007/978-3-319-63537-8_8.

[12] M. Roberts, D. Driggs, M. Thorpe, J. Gilbey, M. Yeung, S. Ursprung, A. I. Aviles-Rivero, C. Etmann, C. McCague, L. Beer et al., "Common pitfalls and recommendations for using machine learning to detect and prognosticate for COVID-19 using chest radiographs and CT scans," *Nat. Mach. Intell.*, vol. 3, no. 3, pp. 199–217, Mar. 2021.

[13] R. M. Pereira, D. Bertolini, L. O. Teixeira, C. N. Silla Jr, and Y. M. Costa, "COVID-19 identification in chest X-ray images on flat and hierarchical classification scenarios," *Comput. Methods Programs Biomed.*, vol. 194, Oct. 2020, Art. no. 105532, DOI: <https://doi.org/10.1016/j.cmpb.2020.105532>.

[14] D. Al-Karawi, N. Polus, S. Al-Zaidi, and S. Jassim, "Artificial Intelligence-Based Chest X-Ray Test of COVID-19 Patients," *Int. J. Comput. Inf. Eng.*, vol. 14, no. 10, 2020, DOI: <https://doi.org/10.1101/2020.05.05.20091561>.

[15] M. A. Elaziz, K. M. Hosny, A. Salah, M. M. Darwish, S. Lu, and A. T. Sahlol, "New machine learning method for image-based diagnosis of COVID-19," *PLoS One*, vol. 15, no. 6, June 2020, Art. no. e0235187, DOI: <https://doi.org/10.1371/journal.pone.0235187>.

[16] A. Z. Khuzani, M. Heidari, and S. A. Shariati, "COVIDClassifier: An automated machine learning model to